The calculated ν_2 (inversion) spectrum of H_3O^+

Di-Jia Liu and Takeshi Oka

Department of Chemistry and Department of Astronomy and Astrophysics, The University of Chicago, Chicago, Illinois 60637

Trevor J. Sears

Department of Chemistry, Brookhaven National Laboratory, Upton, New York 11973

We report the observation and assignment of a number of vibration–rotation transitions within $1^- \leftarrow 1^+$ band of H_3O^+. The data are analyzed together with previously published measurements to yield a consistent set of rotational parameters that accurately reflects the vibration–rotation spectra involving the four lowest levels associated with the ν_2 vibration of the ion. The analysis enables a precise estimate of the inversion splitting and the associated inversion-rotation spectrum of H_3O^+ which occurs in the far infrared.

I. INTRODUCTION

Until two years ago, the only experimental work on the infrared spectrum of the oxonium ion in the gas phase was due to Schwarz[1] who recorded the transient absorption spectra of H_3O^+ and a number of solvated ions around 3 μm following pulse radiolysis of a mixture of water vapor and argon. The resolution of this study was modest and only little structural information could be inferred. Since that time, the situation has changed significantly for two main reasons. Firstly, the development and ready availability of tunable coherent sources of infrared radiation and secondly, the refinement of experimental techniques[2] needed to separate the ion absorptions from the much stronger background of neutral molecule absorption lines. The combination of these advances enabled the first high resolution spectrum of the ion to be detected by Begemann et al.[3,4] who reported the observation and detailed analysis of the ν_3 band spectrum around 3 μm using a color center laser based system.

Spectroscopically, much interest has centered on the ν_2, umbrella, vibration of the ion. As is the case in the isoelectronic ammonia molecule, H_3O^+ has a pyramidal equilibrium structure but the potential function for the out of plane mode has a rather low barrier to inversion. Under these circumstances, the vibrational energy levels associated with the ν_2 mode are split by inversion tunneling through the barrier to planarity. Figure 1 shows the effective inversion potential function and positions of the lowest few vibrational levels as determined recently[5] from data for both H_3O^+ and D_3O^+. In H_3O^+, rotational lines in all of the allowed vibrational transitions indicated have now been observed. In the infrared region, the $1^- \leftarrow 0^+$ band lies at around 10 μm and was detected by Haese and Oka[6] very shortly after the first report of the observation of the ν_3 band by Begemann et al.[3] Subsequently[7,8] other workers reported additional measurements on the 10 μm band and measurements of the 1^+–0^- band at around 20 μm.[8,9] Very recently, Liu and Oka[10] reported the observation of the $1^- \leftarrow 1^+$ hot band of the ion allowing an accurate determination of the inversion splitting for the first time. Following the infrared work, two groups have reported measurements in the mm wave region[11,12] corresponding to rotational transitions in the inversion spectrum $(0^- \leftarrow 0^+)$.

In the present paper, we report the measurement of further transitions in the $1^- \leftarrow 1^+$ band at 20–25 μm and we collect together all of the previously published data relating to the levels shown in Fig. 1, in order to extract a consistent set of molecular parameters describing the rotational energy structure of the ion in these states. The results are compared to theoretical predictions and used to predict additional transitions in the inversion spectrum in the far infrared region. Accurate predictions of these frequencies are necessary because the tunability of currently available FIR sources is limited and extended searching is difficult and time consuming. It is also likely that observations in the FIR will provide a means of detecting H_3O^+ in the interstellar medium where it is thought to be among the most abundant molecular ions.[13,14]

$(\sqrt{3}/2) \sin \rho = \sin(\alpha/2)$
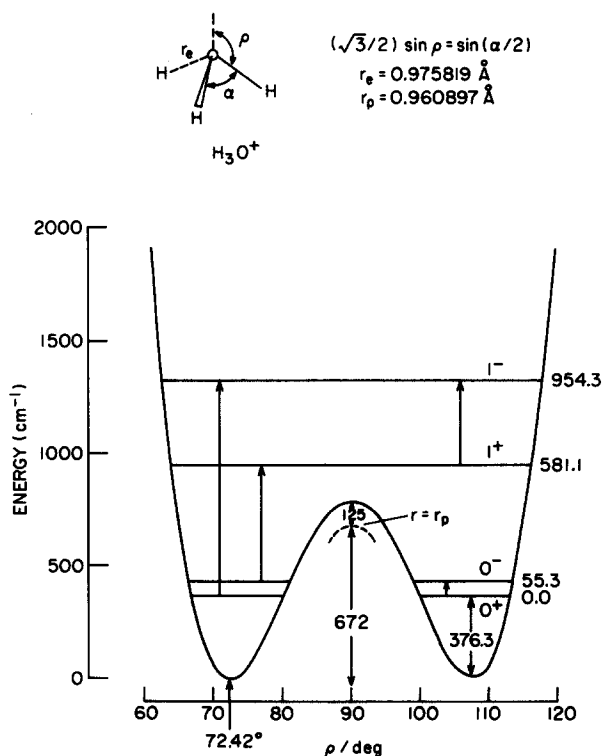$r_e = 0.975819$ Å
$r_p = 0.960897$ Å

H_3O^+

FIG. 1. The inversion potential function of the H_3O^+ ion showing the lowest four vibrational levels and the transitions discussed in the present work.

II. EXPERIMENTAL

The experimental techniques used to record the spectra have been fully described elsewhere[9,15] and only a short account is given here. At the University of Chicago, ion lines were measured using the velocity modulation[2] technique. H_3O^+ was formed in an ac glow discharge in a mixture of H_2O or O_2 and H_2. The optimized mixing ratios were found to be $[H_2O]:[H_2] = 1:4$ and $[O_2]:[H_2] = 1:8$ at a total pressure of 1.8 Torr. The gas mixture was pumped continuously through the water cooled discharge tube which was 80 cm long and had a 1.2 cm internal diameter. The discharge was powered by an audio amplifier stepped up through a transformer and the ion absorption lines were detected by lock-in amplification at the discharge excitation frequency of around 3 kHz. Additional lines were measured at Brookhaven National Laboratory. In this case, the H_3O^+ ions were detected in a hollow cathode discharge[15] in a mixture of H_2 (300 mT) and H_2O or O_2 (10–20 mT). The hollow cathode was operated water cooled at a temperature of about 10 °C and the discharge was powered by a similar amplifier/transformer arrangement at a frequency of 9.6 kHz. Slow pumping was found to be necessary in order to maintain a stable, spike-free discharge current cycle.

The infrared radiation source was provided by diode lasers supplied by Laser Analytics, Inc. The coverage at the low frequency end of the spectrum, i.e., at wavelengths longer than 20 μm, was relatively poor and several diodes of the same nominal operating frequency range were necessary in order to obtain adequate coverage. Even so, there were considerable gaps in the frequencies available. Ion absorption lines were measured relative to SO_2,[16] CS_2 and $^{13}CS_2$,[17] and frequencies and should be accurate to better than 0.001 cm⁻¹ in the most favorable cases.

III. RESULTS AND DISCUSSION

We have measured a significant number of additional lines in the $1^-\leftarrow 1^+$ and 1^+–0^- bands of H_3O^+. Examples of the observed spectra are shown in Figs. 2 and 3 and the observed line wave numbers are given in Table I together with all of the previously reported measurements involving the ν_2 vibration of the ion.[6-12] Some lines have been measured by more than one group, and an average position is quoted in the table except in one or two cases where there were obvious discrepancies. The ν_2 spectrum of H_3O^+ is an example of a parallel vibrational band of a symmetric top molecule[18] and allowed transitions obey the rotational selection rules $J',K \leftarrow J,K$ with $J' = J - 1, J, J + 1$ corresponding to P, Q, and R branches, respectively. The transition frequencies for a particular band are given by

$$\nu(J,K) = \nu_o + [(C' - B') - (C - B)]K^2$$
$$- (D'_K - D_K)K^4 + B'J'(J' + 1)$$
$$- [D'_{JK}K^2 + D'_J J'(J' + 1)]$$
$$\times J'(J' + 1) - BJ(J + 1)$$
$$+ [D_{JK}K^2 + D_J J(J + 1)]J(J + 1). \qquad (1)$$

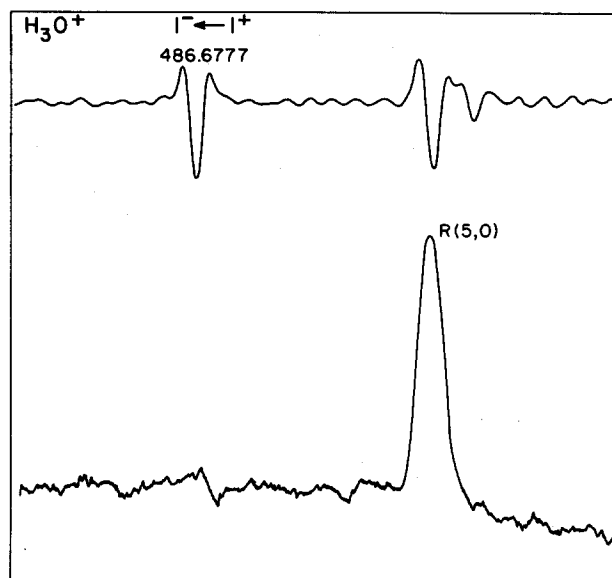FIG. 2. The $R(5,0)$ line in the $1^-\leftarrow 1^+$ band of H_3O^+ observed using the hollow cathode discharge and recorded with an amplifier time constant of 400 ms. The upper trace shows the spectrum of SO_2 in the same region recorded simultaneously and used for frequency calibration.

Here, J and K are the rotational quantum numbers, ν_0 is the band origin, and B, C, and D are the rotational constants and quartic centrifugal distortion constants respectively.

Initially, all of the infrared data were accorded equal weight in the least squares fit to expressions of the form given by Eq. (1) while the mm wave data[11,12] were given a weight 100 times greater. It was found that several of the reported infrared measurements were not in accord with the rest of the data and these were assigned zero weight in the final analysis. Some of these points had already been noted as poorly fitting by Davis et al.[8] however we found that many of the high frequency measurements quoted by these authors
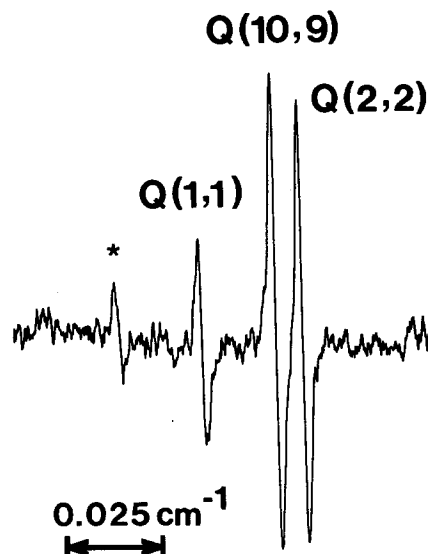

FIG. 3. Group of lines close to the origin of the 1^-–1^+ band. The derivative shape is due to the velocity modulation technique (Ref. 2). The line marked with an asterisk is not assigned. Time constant used was 3 s.

TABLE I. Observed line positions in the $1^-\leftarrow0^+$, $1^+\leftarrow0^-$, $1^-\leftarrow1^+$, and $0^-\leftarrow0^+$ bands of H_3O^+.

(a) $1^-\leftarrow0^+$ Band

P(9,8)[b,g]	756.511(−)	Q(4,3)[b]	949.495(− 3)	R(3,0)[c]	1033.281(− 2)
P(8,6)[b]	769.055(7)	Q(3,2)[c]	950.499(− 4)	R(3,1)[c,g]	1033.963(−)
P(7,6)[b]	798.633(2)	Q(2,1)[b,c]	951.763(− 1)	R(3,3)[c]	1039.391(3)
P(6,3)[b]	809.937(7)	Q(13,12)[b,c]	951.778(4)	R(4,1)[d]	1050.952(− 2)
P(5,0)[c]	831.709(9)	Q(2,2)[b,c]	953.806(− 1)	R(4,2)[d]	1052.920(− 5)
P(4,1)[c]	858.779(− 1)	Q(3,3)[b,c]	953.899(0)	R(4,3)[d]	1056.261(− 6)
P(4,3)[c]	864.008(0)	Q(1,1)[b,c]	953.975(1)	R(5,0)[d]	1066.348(8)
P(3,1)[c]	844.365(− 1)	Q(4,4)[b,c]	954.252(1)	R(5,1)[d]	1066.978(7)
P(3,2)[c]	886.359(− 1)	Q(5,5)[c]	954.867(1)	R(5,3)[d]	1072.124(− 1)
P(1,0)[b]	931.897(0)	Q(6,6)[b,c]	955.751(2)	R(7,1)[d]	1096.391(− 8)
Q(4,2)[b]	946.182(− 4)	Q(7,7)[b]	956.908(1)	R(8,1)[b,g]	1109.961(−)
Q(8,7)[b]	947.968(− 6)	Q(8,8)[c]	958.352(5)	R(7,6)[b,g]	1118.419(−)
Q(7,6)[b,c]	947.980(− 3)	Q(9,9)[c]	960.083(3)	R(9,3)[b,g]	1127.187(−)
Q(9,8)[b,c]	948.213(− 2)	Q(10,10)[b,c]	962.120(3)	R(10,1)[b,g]	1135.362(−)
Q(6,5)[b,c]	948.237(− 3)	Q(11,11)[b,c]	964.473(0)	R(10,3)[b,g]	1139.372(−)
Q(3,1)[b]	948.493(− 5)	Q(12,12)[c]	967.158(− 4)	R(11,1)[b,g]	1147.401(−)
Q(10,9)[c]	948.705(− 3)	R(1,0)[c]	996.064(1)	R(10,5)[b,g]	1147.823(−)
Q(5,4)[c]	948.742(− 3)	R(2,2)[c]	1017.951(1)	R(11,3)[b,g]	1151.128(−)
Q(11,10)[b]	949.458(− 3)				

(b) $1^+\leftarrow0^-$ Band

P(7,2)	377.170(− 1)	Q(4,4)[b,c]	524.356(− 2)	Q(10,6)[b,g]	532.040(−)
P(7,1)	378.123(− 2)	Q(6,5)[b,c]	524.920(2)	Q(9,5)[b,g]	532.076(−)
P(5,3)	415.920(2)	Q(3,3)[b,c]	525.092(− 2)	R(0,0)[c]	548.187(− 2)
P(3,2)[c]	459.317(− 3)	Q(9,7)[c]	525.169(3)	R(1,1)[c]	570.549(6)
P(3,1)[c]	460.110(− 6)	Q(2,2)[c]	525.583(− 2)	R(2,1)[c]	593.383(4)
Q(12,12)[c]	510.775(4)	Q(5,4)[b,c]	525.647(− 3)	R(2,0)[c]	593.637(5)
Q(11,11)[b,c]	513.093(2)	Q(1,1)[b,c]	525.833(3)	R(3,2)[c]	615.691(3)
Q(13,12)[c]	513.379(− 8)	Q(4,3)[c]	526.132(− 1)	R(3,1)[c]	616.454(3)
Q(10,10)[c]	515.270(2)	Q(2,1)[c]	526.347(− 1)	R(4,3)[b]	637.707(− 4)
Q(13,11)[c,g]	518.863(−)	Q(3,2)[c]	526.366(0)	R(4,2)[c]	638.990(5)
Q(8,8)[b,c]	519.113(− 2)	Q(7,5)[b]	526.845(4)	R(4,1)[b,c]	639.772(3)
Q(7,7)[b]	520.751(− 1)	Q(11,8)[b]	527.244(5)	R(4,0)[b,c]	640.040(7)
Q(12,10)[b]	520.809(4)	Q(6,4)[b]	527.300(3)	R(5,5)[b]	657.259(− 4)
Q(9,8)[b]	521.272(− 2)	Q(4,2)[b]	527.450(3)	R(5,4)[b]	659.442(− 1)
Q(6,6)[b,c]	522.178(− 1)	Q(5,3)[b]	527.499(0)	R(5,3)[b]	661.223(− 1)
Q(11,9)[b]	522.500(3)	Q(9,6)[b,c]	528.809(− 10)	R(5,1)[b]	663.345(− 8)
Q(8,7)[b,c]	522.724(1)	Q(5,2)[b,c]	528.864(− 1)	R(9,8)[b]	743.398(1)
Q(5,5)[c]	523.384(0)	Q(8,5)[c]	529.218(2)	R(9,5)[b,g]	753.545(−)
Q(7,6)[b]	532.934(− 6)	Q(6,3)[c]	529.238(4)	R(10,9)[b]	763.651(2)
Q(10,8)[b]	532.949(− 4)	Q(8,4)[b,g]	531.865(−)	R(11,11)[b]	779.383(− 2)

(c) $1^-\leftarrow1^+$ Band

Q(1,1)[e]	372.913(1)	R(1,1)	415.687(− 1)	R(7,3)[f]	522.440(2)
Q(10,9)[e]	372.933(− 8)	R(4,1)	470.944(− 3)	R(6,6)[f]	525.801(− 1)
Q(2,2)[e]	372.941(− 1)	R(4,2)	472.923(− 1)	R(7,4)	527.027(1)
Q(3,3)[e]	373.324(9)	R(4,3)	476.216(− 3)	R(8,1)	530.635(5)
Q(12,11)[e]	376.621(− 7)	R(4,4)	480.835(− 1)	R(7,6)	540.161(1)
Q(7,7)[e]	378.154(2)	R(5,0)	486.704(− 2)	R(8,4)	540.429(4)
Q(13,12)[e]	378.910(7)	R(5,1)	487.362(− 1)	R(9,2)[e]	545.028(− 1)
Q(8,8)[e]	380.174(3)	R(5,2)[e]	489.336(− 1)	R(9,3)[e]	548.287(1)
Q(9,9)[e]	382.496(− 3)	R(6,3)	508.033(1)	R(7,7)[e]	548.718(4)
R(1,0)	415.026(− 3)	R(7,2)[f]	519.165(3)	R(8,6)[f]	553.519(4)

(d) $0^-\leftarrow0^+$ Band

P(2,1)[b,i]	10.246 82(0)	P(3,1)[i,j]	− 12.957 57(0)
P(3,2)[i,j]	− 12.168 31(0)	P(3,0)[i,j]	− 13.218 21(0)

[a] In cm^{-1}. Numbers in parentheses are $10^3 \times$ the observed-calculated frequencies using the parameters given in Table II. Where frequencies are derived from more than one source, the average is given.
[b] Reference 8.
[c] Reference 9.
[d] Reference 7.
[e] Reference 10.
[f] P. B. Davies, private communication.
[g] Line not in accord with the rest of the data and given weight of zero in final analysis.
[h] Reference 11.
[i] Line given relative weight of 100.
[j] Reference 12.

gave problems in the fitting. These represent the information on the highest lying rotational levels in the data set and the problems encountered here could in part be due to our neglect of higher order centrifugal distortion terms in Eq. (1). We do not feel that this is the entire explanation however, and think that there may be an absolute frequency calibration error in these measurements.

The standard deviation of the final fit was 0.004 cm^{-1} which is adequate but not outstanding. Individual measurements should be significantly better than this and the fit probably reflects problems in the absolute frequency calibrations of the FTIR spectra used as wavelength standards for the various bands. Fits of lower standard deviation could be achieved if higher order centrifugal distortion constants were allowed to vary, however the resulting parameters were only marginally determined and since there are no obvious systematic trends in the residuals given in Table I, it was not clear which higher order parameters should be introduced. We believe that the parameters given in Table II represent a good compromise and they can be used to predict the vibration–rotation spectrum of the ion over the large range of rotational quantum numbers included in the data set.

Also in Table II we give parameters derived from two theoretical studies[19,20] and those derived by Begeman and Saykally[4] from the analysis of the ν_3 band. It is difficult to overemphasize the contributions made by the various theoretical groups[19-21] in the initial stages of the spectroscopic measurements of this ion. In the ν_2 band region where available diode laser sources suffer from limited tuning range and incomplete frequency coverage, theoretical guidance was crucial to the successful observation of the H_3O^+ spectrum. The nonrigid invertor calculations by Bunker and co-workers[19,20] provided what have proved to be exceptionally good estimates of the rotational parameters which allowed the fragmentary spectral information to be assigned.

The derived parameters for the $0^- \leftarrow 0^+$ band allow us to make a reliable estimate of the inversion doubling spectrum of the ion. This occurs in the far infrared region of the spectrum where available radiation sources are currently poor in terms of power and tunability, however as experimental techniques improve it is certain that the spectrum will be observed. In Table III we list the low J spectrum as calculated using the parameters given in Table II. The Q-branch region of the spectrum is very congested and should provide a distinctive spectral signature for the ion.

The present parameters are the best currently available for the H_3O^+ ion and any significant improvement will require the direct observation of the rotation inversion spectrum given in Table III. It is interesting to note that the parameters in Table II yield markedly different predictions for the higher J R-branch transitions when compared to those based on the parameters given by Liu and Oka.[10] Some of these transitions occur at frequencies accessible by currently available diode lasers and Liu and Oka[10] assigned several lines around 380 cm^{-1} to this type of transition. However, these are now predicted to lie several wave numbers

TABLE II. Molecular constants of H_3O^+ (in cm^{-1}).

Quantity	This work	BKS[a]	BAS[b]	BS[c]
$\nu_0(1^- \leftarrow 0^+)$	954.400 1(12)[d]	992.	954.4	
$\nu_0(1^+ \leftarrow 0^-)$	525.826 6(11)	511.	543.5	
$\nu_0(1^- \leftarrow 1^+)$	373.225 4(13)	409.	363.4	
$\nu_0(0^- \leftarrow 0^+)$	55.348 1(21)	72.	47.5	
$[(C-B)(1^-)]-[(C-B)(0^+)]$	0.686 49(12)	0.67	0.69	
$[(C-B)(1^+)]-[(C-B)(0^-)]$	-0.251 80(11)	-0.20	-0.34	
$[(C-B)(1^-)]-[(C-B)(1^+)]$	0.656 86(10)	0.56	0.74	
$[(C-B)(0^-)]-[(C-B)(0^+)]$	0.281 43(19)	0.31	0.29	
$B(1^-)$	10.697 41(12)	10.66	10.71	
$B(1^+)$	11.182 47(14)	11.03	11.24	
$B(0^-)$	11.054 86(14)	10.94	11.06	
$B(0^+)$	11.253 97(15)	11.14	11.26	11.2463(16)
$D_J(1^-)$	5.16(2)[e]	7.2	10.49	
$D_J(1^+)$	6.37(3)	6.7	10.83	
$D_J(0^-)$	10.04(2)	9.0	12.41	
$D_J(0^+)$	13.08(3)	11.0	15.83	11.13(25)
$D_{JK}(1^-)$	-5.87(5)	-10.7	-16.07	
$D_{JK}(1^+)$	-7.97(6)	-8.3	-16.03	
$D_{JK}(0^-)$	-18.48(5)	-16.7	-22.58	-22.90(57)
$D_{JK}(0^+)$	-26.91(8)	-22.5	-32.08	
$D_K(1^-)-D_K(0^+)$	-13.85(3)	-9.2	-11.67	
$D_K(1^+)-D_K(0^-)$	-7.69(3)	-7.0	-6.09	
$D_K(1^-)-D_K(1^+)$	-0.42(2)	2.2	0.97	
$D_K(0^-)-D_K(0^+)$	-5.74(7)	-4.4	-6.55	

[a] Theoretical prediction; Ref. 19.
[b] Theoretical prediction; Ref. 20.
[c] Reference 4.
[d] Numbers in parentheses are one standard deviation of the least squares fit in units of the last quoted significant figure.
[e] Centrifugal distortion constants in units of 10^{-4} cm^{-1}.

TABLE III. The calculated inversion spectrum of H_3O^+.[a]

(J,K)	P	Q	R
5,5	...	56.4107	188.7559
5,4	− 56.4487	53.8936	186.0393
5,3	− 58.2128	52.0002	183.9906
5,2	− 59.4384	50.6821	182.5617
5,1	− 60.1600	49.9051	181.7182
5,0	− 60.3982	...	181.4393
4,4	...	55.8676	166.2098
4,3	− 34.3998	53.9151	164.1280
4,2	− 35.6860	52.5550	162.6755
4,1	− 36.4440	51.7526	161.8177
3,3	...	55.4909	143.8058
3,2	− 12.1681[c]	54.0970	142.3380
3,1	− 12.9574[c]	53.2744	141.4711
3,0	− 13.2182[c]	...	141.1844
2,2	...	55.2791	121.5441
2,1	10.2466[b]	54.4413	120.6732
1,1	...	55.2314	99.4261
1,0	32.8454	...	99.1384

[a] In cm^{-1}, calculated using the parameters in Table II. Where the frequency is negative, the 0^+ rotational level lies above the 0^- one.
[b] Transition observed by Plummer et al. (Ref. 11).
[c] Transition observed by Bogey et al. (Ref. 12).

away from the reported frequencies, indicating that reassignments at least are necessary. Realistically, even the current set of parameters cannot be expected to accurately predict transitions where the average rotational quantum number is 15. Considerably more observations are necessary before reliable assignments can be made.

IV. SUMMARY

We have reported the observation and assignment of a number of new transitions in the $1^- \leftarrow 1^+$ band of H_3O^+. Using these in conjunction with previously reported data, we have derived a reliable set of molecular parameters for the ion that can be used to calculate vibration–rotation band structure involving the lowest four vibrational levels associated with the inversion mode. The parameters are used to calculate the inversion-rotation spectrum around 50 cm^{-1}. Future work will involve measurements of rotation–vibration bands involving higher lying vibrational levels, indeed many transitions in the 2^+–1^- band have already been observed.[22] Such measurements will enable the potential function for the inversion motion to be more accurately determined. By analogy with ammonia, the 2^+ level is predicted to be perturbed by the $v_4 = 1$ vibrational level through Coriolis interactions and detailed observations of 2^+–1^- could provide information on the latter state which has yet to be observed experimentally.

ACKNOWLEDGMENTS

[1] H. A. Schwarz, J. Chem. Phys. 67, 5525 (1977).
[2] C. S. Gudeman, M. H. Begemann, J. Pfaff, and R. J. Saykally, Phys. Rev. Lett. 50, 727 (1983).
[3] M. H. Begemann, C. S. Gudeman, J. Pfaff, and R. J. Saykally, Phys. Rev. Lett. 51, 554 (1983).
[4] M. H. Begemann and R. J. Saykally, J. Chem. Phys. 82, 3570 (1985).
[5] T. J. Sears, P. R. Bunker, P. B. Davies, S. A. Johnson, and V. Špirko, J. Chem. Phys. 83, 2676 (1985).
[6] N. N. Haese and T. Oka, J. Chem. Phys. 80, 572 (1984).
[7] B. Lemoine and J. L. Destombes, Chem. Phys. Lett. 111, 284 (1984).
[8] P. B. Davies, P. A. Hamilton, and S. A. Johnson, J. Opt. Soc. Am. B 2, 794 (1985).
[9] D.-J. Liu, N. N. Haese, and T. Oka, J. Chem. Phys. 82, 5368 (1985).
[10] D.-J. Liu and T. Oka, Phys. Rev. Lett. 54, 1787 (1985).
[11] G. M. Plummer, E. Herbst, and F. C. DeLucia, J. Chem. Phys. 83, 1428 (1985).
[12] M. Bogey, C. Demuynck, M. Denis, and J. L. Destombes, Astron. Astrophys. 148, L11 (1985).
[13] E. Inglesias, Astrophys. J. 218, 697 (1977).
[14] S. S. Prasad and W. T. Huntress, Jr., Astrophys. J. Suppl. 43, 1 (1980).
[15] T. J. Sears, J. Opt. Soc. Am. B 2, 786 (1985).
[16] We are grateful to S. C. Foster and J. W. C. Johns of the Herzberg Institute of Astrophysics for providing us with the SO_2 spectrum used for frequency calibration.
[17] K. Jolma and J. Kauppinan, J. Mol. Spectrosc. 82, 214 (1980); J. Kauppinan and K. Jolma, ibid. 85, 314 (1981).
[18] G. Herzberg, Molecular Spectra and Molecular Structure. Vol. III. Electronic Spectra and Electronic Structure of Polyatomic Molecules (Van Nostrand, New York, 1966).
[19] P. R. Bunker, W. P. Kraemer, and V. Špirko, J. Mol. Spectrosc. 101, 180 (1983).
[20] P. R. Bunker, T. Amano, and V. Špirko, J. Mol. Spectrosc. 107, 208 (1984).
[21] P. Botschwina, P. Rosmus, and E.-A. Reinsch, Chem. Phys. Lett. 102, 29 (1981).
[22] P. B. Davies, P. A. Hamilton, S. A. Johnson, and T. J. Sears (unpublished data).